



OVERCURRENT PROTECTIVE RELAYS FOR ELECTRIC DISTRIBUTION SYSTEMS

AUTHORS:

A. E. Anyalebechi^{1*}, and B. O. Anyaka²

AFFILIATIONS:

¹Department of Electrical Engineering, Nnamdi Azikiwe University, Nigeria.

²Department of Electrical Engineering, University of Nigeria, Nigeria.

*CORRESPONDING AUTHOR:

Email: ae.anyalebechi@unizik.edu.ng

ARTICLE HISTORY:

Received: 19 March, 2024.

Revised: 03 September, 2024.

Accepted: 27 September, 2024.

Published: 31 December, 2024.

KEYWORDS:

Numerical, Electromechanical, micro-controller, over-current, relay, electric feeder.

ARTICLE INCLUDES:

Peer review

DATA AVAILABILITY:

On request from author(s)

EDITORS:

Ozoemena Anthony Ani

FUNDING:

None

Abstract

This paper presents over-current protective relays for electric distribution systems. The objective is to determine the reliability of the system by comparing the performance of numerical and electromechanical relays. Electromechanical over-current protective relay on 33kV Itire-Ijesha distribution feeder was analyzed and modeled using MATLAB/Simulink. A numerical relay was proposed and also modeled using the real data of the existing Itire-Ijesha 33kV distribution feeder. While electromechanical relay was simulated as an instantaneous relay, the numerical relay was programmed and simulated as an IEEE moderately inverse definite minimum time (IDMT) relay. The simulation was for single line-to-ground fault with the red phase, double line-to-ground fault using red and blue phase as well as line-to-line fault using red and blue phase. Comparing the performances of the two different models, numerical relay tripped in mini-seconds while the electromechanical relay model tripped in seconds. In conclusion, therefore, the numerical relay proved to be superior, smarter, and more reliable than electromechanical relays.

1.0 INTRODUCTION

Power system protection is generally aimed at controlling failure modes so as to limit damage and enhance reliability [1]. The importance of power system over-current protection cannot be overemphasized. In every engineering practice safety is paramount and of utmost necessity. Over-current flow in conductors or electrical components will cause damage and ultimately lead to high cumulative ohmic losses. Utility companies aim towards continuous supply of quality electricity to their customers. But whenever fault occurs, with inherent over-current flow, it will definitely interrupt the smooth operation of the power system. This will definitely lead to different kinds of losses such as revenue loss, property loss, man-hour loss in terms of time lapse before repair, and so on. Therefore, there is every need to ensure continuous quality power supply to consumers. The desire to avoid revenue loss as well as other disadvantages due to system failure necessitated further research aimed towards improving over-current protection. However, increasing complexity of power systems makes it difficult for conventional protection operations to achieve this objective and this has necessitated the introduction of numerical relays. The superiority of these relays is evident in their high speed and accuracy in data processing [2].

HOW TO CITE:

Anyalebechi, A. E., and Anyaka, B. O. "Overcurrent Protective Relays for Electric Distribution Systems", *Nigerian Journal of Technology*, 2024; 43(4), pp. 772 – 778; <https://doi.org/10.4314/njt.v43i4.17>

© 2024 by the author(s). This article is open access under the CC BY-NC-ND license

Over-current protective relays can be classified into three major types according to their construction: electromechanical, static, and digital (numerical) relays [3]. An electromechanical relay operates by using a magnetic field that emanates from an electromagnetic coil when some current is applied to it. The name electromechanical is because it has parts that move when the right signal is applied. In addition to this, a switch which is electrically operated and does not have a moving part is called a static relay. Some common types of static relays include electronic relays, transducer relays, transistor relays, rectifier bridge relays, and Gauss effect relays. Digital relays, on the other hand, use the switching algorithm installed in their microprocessor to analyze parameters such as voltage, current, frequency, before making tripping decision. They have no moving parts and they are very smart. The original contribution of this paper is a design of a novel numerical over-current protective relay that will enhance the reduction of ohmic losses (I^2R) on the Power systems generally.

In “Highly sensitive microgrid protection using over-current relays with a novel relay characteristic”, interest was focused on optimal over-current coordination improvement under faulty conditions in the presence of synchronous generators. A new over-current relay curve was proposed to reduce the operating time of the over-current relay. However, the use of combinatorial optimization method and synchronous generator sizing and location made this exercise cumbersome. Since source impedance is often constant from power distribution perspective, inverse definite minimum time characteristic still gives better results [4]. In “Distribution system protection by coordinated fault current limiters” interest was focused on the protection of power distribution networks using fault current limiters. One major disadvantage of using fault current limiter in the over-current protection of distribution networks is the introduction of resistance and additional power losses. In our proposed numerical relay there is no additional power loss introduced [5]. In “Adaptive over-current relay (AOCR) based on Fano Factors of current signal” a scheme of adaptive over-current protection was presented. The same mathematical algorithm was used to estimate Fano Factors (FFs) of current signals so as to determine the operating time. In our proposed inverse definite minimum time (IDMT) relay operating time is dependent on the exact value of the fault current which makes the scheme simple and accurate [6].

In “Settings determination for numerical transformer differential protection via its detailed mathematical

model” the authors presented a novel approach for relay protection settings determination to ensure its correct operation in the presence of transients in faulty conditions. But in our proposed scheme metal oxide varistors (MOVs) are used to suppress transients and ensure that current signals that enter the anti-aliasing filter are clean and devoid of useless harmonics. MOVs are also cost effective [7]. In “A new relaying scheme for protection of transmission lines connected to doubly-fed induction generator-based wind farms” a new protection scheme was presented. Here, an attempt was made to solve the problem of non-synchronous frequency component of the current fed from a doubly-fed induction generator-based wind farm during a short circuit fault. Again, in our proposed IDMT relay, non-synchronous frequency components of the current are completely eliminated by the anti-aliasing filter before reaching the sample-and-hold circuit [8].

Furthermore, another research work, Integrated busbar protection scheme utilizing a numerical technique based on coherence method is based on closed-tripping characteristics of coherence coefficients computed for busbar current signals. However, this proposed scheme was not tested with real data of any known existing network [9]. In addition to this, in “Optimal coordination of directional over-current relays using improved mathematical formulation” a new objective function was proposed so as to achieve optimum coordination of directional over-current relays. The simple target here is to minimize the operating time of primary and backup relays as well as the discrimination time between their operations. This was formulated using genetic algorithm but was not tested with any real data [10]. Asma Soleimanisardoo and Hossein Kazemi Karegar also researched on “Alleviating the impact of distributed generators (DGs) and network operation modes on the protection system”. According to the authors, integration of distributed generators into the distribution network leads to a significant change of fault current behavior in magnitude and direction which may affect the relay setting. Though our proposed scheme is aimed at over-current protection of radial distribution feeders, fault current direction will not affect the relay settings [11].

2.0 METHODOLOGY (ANALYSIS AND MODELING OF ELECTROMECHANICAL OVER-CURRENT PROTECTION RELAY)

The Itire-Ijsha 33kV line is approximately 80km and therefore, can be modelled as a short transmission line. In modelling short transmission lines, the shunt



capacitance can be ignored. Hence, the formula for short line modelling is as follows:

$$Z = (r + j\omega L)\iota \tag{1}$$

$$= R + jX \tag{2}$$

The letter r stands for the per-phase resistance per unit length while the letter L stands for the inductance per unit length. The letter ι stands for the total line length and ω is the angular velocity. Also, Z represents the series impedance per unit length. Figure 1 shows the per-phase short line model of Itire-Ijesha 33kV distribution feeder. V_S represents the phase voltage at the sending end while I_S represents the phase current at the sending end. In addition to this, V_R represents the phase voltage at the receiving end while I_R represents the phase current at the receiving end.

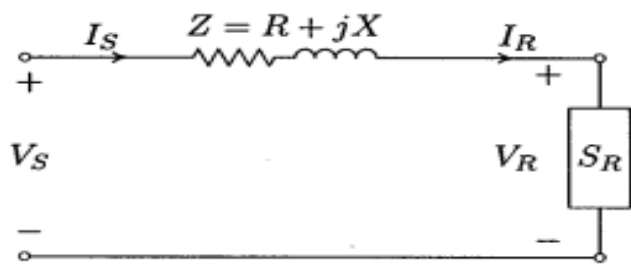


Figure 1: Short line Model of Itire-Ijesha 33kV line

For the conductor (Wolf) used for the Itire-Ijesha feeder $r = 0.1871\Omega/\text{km}$; $L = 1.0377 \text{ mH}/\text{km}$; $\omega = 314.16 \text{ rads/s}$; and $\iota = 80\text{km}$. Hence,
 $Z = [0.1871 + j(2\pi \times 50 \times 1.0377 \times 10^{-3})]80$
 $= (15 + j26) \Omega = 30\angle 600 \Omega$

The receiving end phase voltage is V_R . Hence,

$$V_R = \frac{33 \times 10^3}{\sqrt{3}} = 19\text{kV} = 19\angle 0^\circ \text{ kV}$$

Receiving end apparent power (real data from field) is S_R . Hence,

$$S_R = 18\text{MVA} = 18\angle \cos^{-1}0.8$$

$$= 18\angle 36.87^\circ \text{ MVA}$$

Recall that, $S_R^* = 3I_R V_R^*$, where S_R^* is the conjugate value of the receiving end apparent power and the current per phase is I_R . Hence,

$$I_R = \frac{S_R^*}{3V_R^*} = \frac{18\angle -36.87^\circ \times 10^6}{3 \times 19\angle 0^\circ \times 10^3}$$

$$= 315.8\angle -36.87^\circ \text{ A (recall, } I_R = I_S)$$

The sending end phase voltage is given by

$$V_S = V_R + I_R Z$$

$$= 19 \times 10^3 \angle 0^\circ + (315.8\angle -36.87^\circ \times 30\angle 60^\circ)$$

$$= 27965.5\angle 7.66^\circ \text{ V}$$

$$= 28.0\angle 7.7^\circ \text{ kV}$$

The sending end line-to-line voltage is

$$V_{SL} = V_S \times \sqrt{3}$$

$$= 28\angle 7.7^\circ \times \sqrt{3}$$

$$= 48.5\angle 7.7^\circ \text{ kV}$$

Therefore, magnitude of the sending end line-to-line voltage is

$$|V_{SL}| = 48.5 \text{ kV}$$

The sending end apparent power is

$$S_S = 3I_S^* V_S$$

$$= 3 \times 315.8\angle 36.87^\circ \times 28.0\angle 7.7^\circ \times 10^3$$

$$= 26527.2 \times 10^3 \angle 44.57^\circ$$

$$= 26.52\angle 44.57^\circ \text{ MVA}$$

Therefore, the following parameters are some of the existing (real data) and calculated data of Itire-Ijesha distribution line:

1. Receiving end phase voltage $V_R = 19\angle 0^\circ$
2. Apparent receiving end power $S_R = 18\angle 36.87^\circ$
3. Receiving end current per phase $I_R = 315.8\angle -36.87^\circ \text{ A}$ (also, $I_R = I_S$)
4. Sending end voltage $V_S = 28.0\angle 7.7^\circ$
5. Sending end line-to-line voltage $|V_{SL}| = 48.5 \text{ kV}$
6. Sending end power $S_S = 26.52\angle 44.57^\circ \text{ MVA}$
7. Inductance per unit length $L = 1.0377\text{mH}/\text{Km}$
8. Resistance per unit length $R = 0.1871\Omega/\text{km}$
9. The series impedance per phase $Z = 30\angle 60^\circ \Omega$,
10. Real power of load 14.4MW,
11. Reactive power of load 10.8Mvar.

Some of the parameters above were used in the modeling of the source Itire transmission station (TS), feeder line, and the load (Ijesha substation) respectively.

Figure 2 is the simulink model of Itire-Ijesha 33kV distribution feeder with electromechanical over-current protection relay:

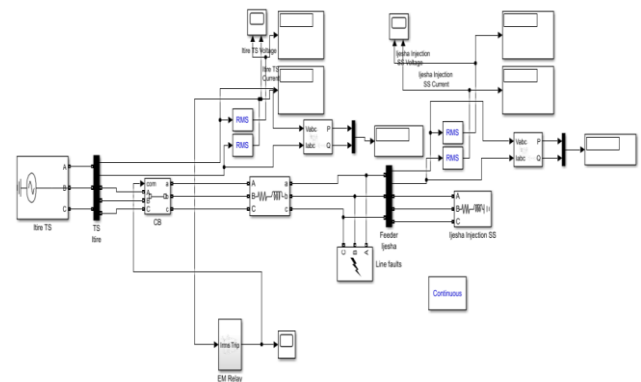


Figure 2: Simulink model of Itire-Ijesha 33kV distribution feeder with EM

Figure 2 shows the schematic connection of the electromechanical relay in the 33kV distribution system. Itire 132/33kV transmission station (TS) is modeled as the source and it is connected through a

series three phase RL lines to the load. Ijessa injection substation is modeled as the load.

3.0 THE PROPOSED MICROCONTROLLER BASED OVER-CURRENT PROTECTION RELAY

Figure 3 shows the circuit diagram of the proposed microcontroller-based over-current protective scheme for Itire-Ijessa 33kV electric distribution system. The components that make up the proposed scheme include:

- i. Current transformer
- ii. Surge arrester
- iii. Second order low pass anti-aliasing filter
- iv. Sample-and-hold circuit
- v. PIC16F877A Microcontroller
- vi. Three phase circuit breaker
- vii. NPN Transistor
- viii. One drelay
- ix. One power system battery
- x. Capacitors
- xi. Resistors
- xii. One liquid crystal display (LCD)

Additional mathematical details of the proposed scheme are shown below Figure 3.

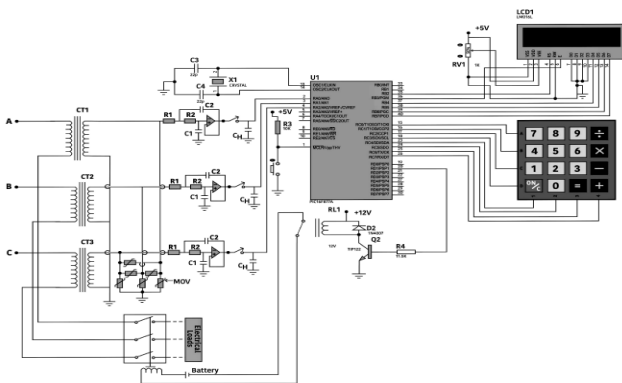


Figure 3: Proposed microcontroller-based over-current protective scheme

We can select a high speed crystal/resonator at 20MHz with C3 and C4 values of 33pF from the datasheet of pic16f877a. The value of the crystal oscillator is selected during the configuration of the analogue pin.

R_3 is calculated using the formula below;

$$R_3 = V_{in} - V_{out} / I_{out}$$

Where, V_{in} is the output voltage of pic16f877a = 5v, V_{out} is the LED voltage given in the datasheet of LED in the range of $1.8v \leq LED \leq 2v$, I_{out} is the LED current given in the datasheet of LED in the range of $10mA \leq LED \leq 20mA$.

Therefore $R_3 = 5 - 2/0.02 = 150\Omega$

Also, $R_3 = R_{v1}$

R_{v1} is used to set the contrast of the LCD which is selected from the datasheet of the LCD. Holding capacitor for the sample-and-hold circuit $C_H = 0.01\mu F$, from the datasheet.

4.0 MODELING OF THE MICROCONTROLLER BASED (NUMERICAL) OVER-CURRENT RELAY

By modeling Itire-Ijessa 33kV line, as shown under Section 2, several parameters were determined. Some of these values were used in building the simulink model of the source (Itire TS), feeder line, and the load (Ijessa substation) shown in Figure 4. The line parameters (R & L) remain the same as we have under electromechanical relay in Section 2. The implementation of the algorithm is done in MATLAB/Simulink environment for the system. The microcontroller block is programmed with a switching code developed based on the IEEE very inverse model equation shown in Equation 3. The code is written with MATLAB scripts.

$$t(I) = TD \left(\frac{A}{\left(\frac{I}{I_c}\right)^p - 1} + B \right) \quad (3)$$

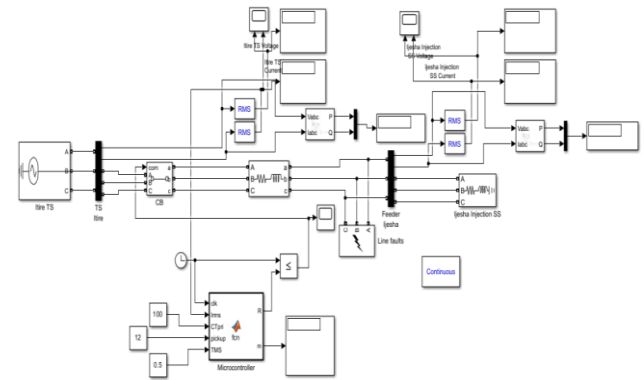


Figure 4: Simulink model of the proposed microcontroller-based IDMT relay

5.0 RESULTS AND DISCUSSION (ELECTROMECHANICAL RELAY OVER-CURRENT PROTECTION SCHEME RESPONSES)

In all the simulations below, both under electromechanical relay and under numerical relay, Red colour represents phase A, Blue colour represents phase B, and Yellow colour represents phase C.

5.1 Single line-to-Ground Fault

The single line-to-ground fault simulated is phase A-to-ground fault. As shown, the fault was activated at 0.4 seconds. In Figure 4, it can be seen that the root mean square (RMS) fault current is about 500A from



about 240A. The effect can also be seen on phase A and phase C of the voltage waveform.

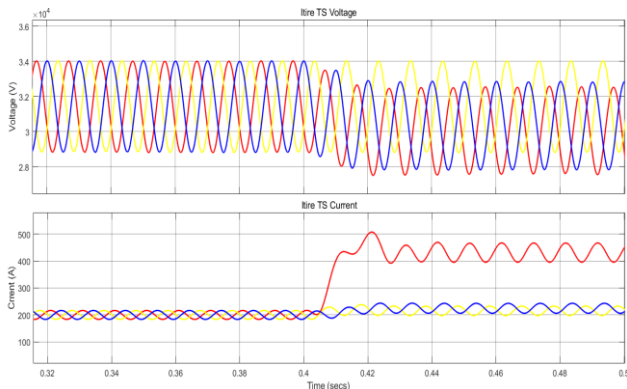


Figure 5: Current and voltage waveforms showing the occurrence of single line-to-ground fault under Electromechanical relay

The operating time was about 4.37 seconds as shown in Figure 5. The maximum fault current as measured on the primary side of the current transformer is 494.1A while the secondary side is 24.71A. However, the average fault current, after the initial spike, on the secondary side of the current transformer is 22.48A (or 449.52A on the primary side). This gives a plug setting multiplier (PSM) of 1.837. The protective relay tripped at 4.81 seconds as shown in Figure 5.

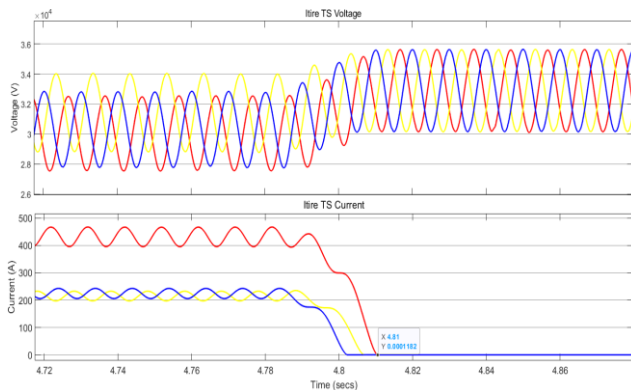


Figure 6: Current and voltage waveforms after clearing the single line-to-ground fault

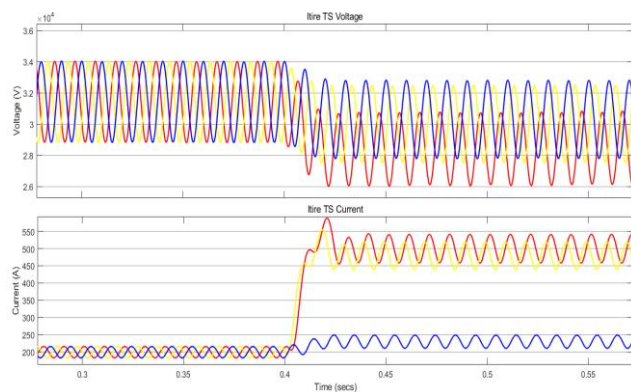


Figure 7: Current and Voltage waveforms showing the occurrence of Line-Line-Ground fault

5.2 Double Line-to-Ground Fault

Phase A and phase B were used for the simulation of double line-to-ground fault. The current and voltage waveforms showing the occurrence of the fault and clearance are shown in Figures 6 and 7.

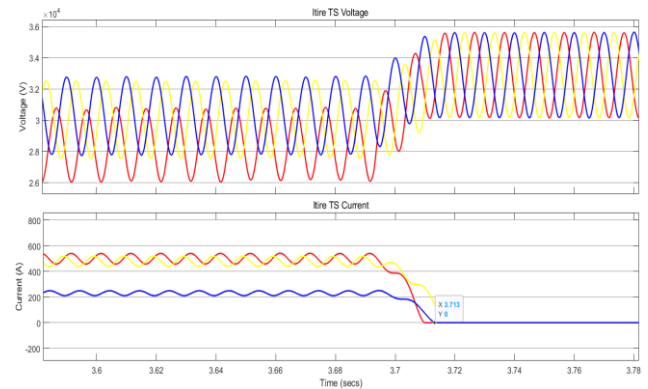


Figure 8: Current and Voltage waveforms after clearing the double line-to-ground fault

5.3 Line-to-Line Fault

Again, phase A and phase B were used for simulating this fault. The voltage and current waveforms showing the occurrence of this fault and the time of isolation are both shown in Figures 8 and 9 below.

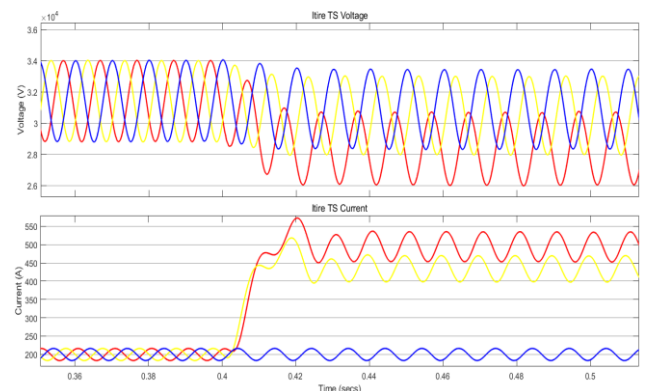


Figure 9: Current and Voltage Waveforms showing the occurrence of double line fault

Figure 10: Current and Voltage waveforms after clearing the double line fault.

6.0 MICROCONTROLLER-BASED OVER-CURRENT PROTECTION SCHEME RESPONSES

Single line-to-ground fault, double line-to-ground fault, and line-to-line fault were simulated. The details of the various simulation results are as shown below.

6.1 Single Line-to-Ground Fault

The single line-to-ground fault simulated is between phase A and ground which was triggered at 0.4 seconds. Figure 10 shows that the peak current increased from 216.3A to 440.1 A after the single line-to-ground fault occurred between line A and the ground. The network was isolated at 0.426 seconds. This implies that the difference between time of fault occurrence and time of network isolation is 0.026 seconds or 26ms.

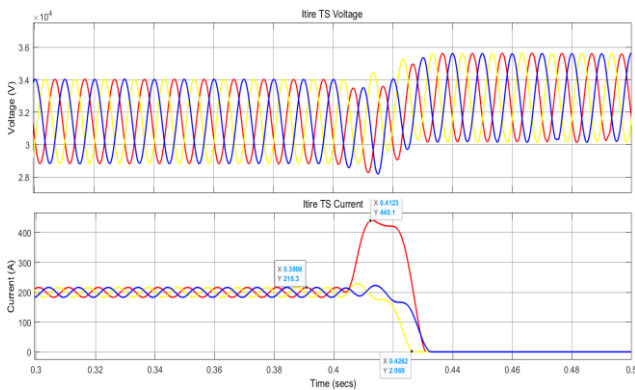


Figure 11: Current and voltage waveforms showing the occurrence and clearance of single line-to-ground fault using numerical relay

6.2 Double Line-to-Ground Fault

The double line-to-ground fault was simulated and the peak current for this fault was 470.7A as shown in Figure 11. The response time was 22.4ms.

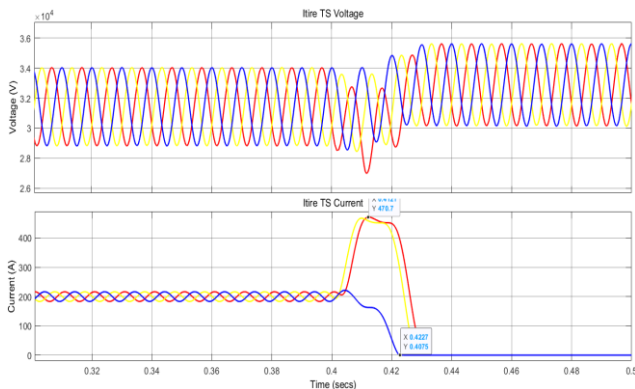


Figure 12: Current and voltage waveforms showing the occurrence and clearance of double line-to-ground

fault using numerical relay

6.3 Line-to-Line Fault

The line-to-line fault was simulated using phase A and phase B. The maximum peak current occurred between phase A and phase B while the current on phase C became zero. The voltage and current waveforms for this fault is shown in Figure 12. However the peak maximum current of 464.3A in line-to-line fault is less than 470.7A in double line-to-ground fault. It took 22.7 ms to isolate the network with numerical relay.

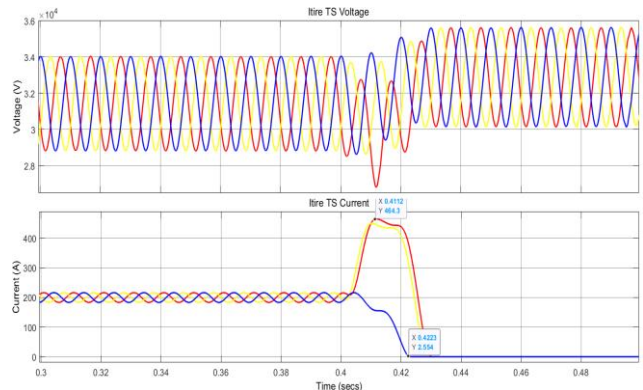


Figure 13: Voltage and current waveforms for line-to-line fault occurrence and clearance under numerical relay

7.0 COMPARISON OF RESPONSES OF NUMERICAL RELAY AND ELECTROMECHANICAL RELAY OVER-CURRENT PROTECTION SCHEMES FOR DIFFERENT LINE FAULTS

Table 1 is a summary of the results of the simulations of the unsymmetrical line faults. Each of the faults was initialized, in a particular scheme, at 0.4seconds. The time gap between the occurrence of each fault and tripping of the circuit breaker is the operating time of the scheme. Table 1 also shows the maximum fault current and operating time for the over-current inverse definite minimum time (IDMT) controller and electromechanical relay for different types of line faults. Single line-to-ground fault has the lowest fault current value and therefore it also has the highest operating time for the circuit breaker.

Table 1: Maximum fault current and operating time for different faults under numerical and electromechanical relays

S/N	TYPE OF FAULTS	MAX. FAULT CURRENTS (A)	OPERATING TIME (seconds)	
			Electromechanical Relay	Numerical Relay
1	Single Line-to-Ground	494.1	4.373	0.026
2	Double Line-to-Ground	564.2	3.287	0.023
3	Line-to-Line	535.9	3.561	0.022

8.0 CONCLUSION

Microcontrollers are intelligent electronic devices capable of performing complex logic or communication tasks. Hence, incorporating them into numerical relays makes the numerical relays superior to electromechanical relays which also have limited functionality. In this paper, we analyzed, modeled, and simulated Itire-Ijesha feeder over-current protective scheme. We then proposed, designed and modeled a numerical over-current protective scheme for the same Itire-Ijesha feeder. From the responses of the two schemes we can conclude that numerical relay is superior to electromechanical relay. Numerical relays also enhance the reduction of I²R losses in the power systems generally by optimal prevention of over-current flow.

REFERENCES

- [1] Awosope, C. A. "Nigeria Electricity Industry: issues, challenges and solutions", Covenant University Public Lecture Series, vol. 3, no. 2, p. 40, 2014.
- [2] Gunasekari, G. R., Mary, D., and Kishoreraja, D. "Performance evaluation of a Modern NPR for Over Current Protection with the Application of Microcontroller Technology in Power System", International Journal of Eng. Research and Development, vol. 10, issue 3, 2014.
- [3] Ramarao, G., Telagamsetti, S. R., and Kale, V. S. "Design of Microcontroller-based Multi-functional Relay for Automated Protective System", Electrical Eng. Dept., Visvesvaraya NIT, Nagpur, India, 2014.
- [4] Darabi, A., Bagheri, M., and Gharehpetian, G. B. "Highly sensitive microgrid protection using overcurrent relays with a novel relay characteristic", IET Review. Power Gener., 2020, vol. 14 issue 7, pp. 1201-1209.
- [5] Heidary, A., Radmanesh, H., Naghibi, S. H., Samandarpour, S., Rouzbehi, K., and Shariati, N. "Distribution system protection by coordinated fault current limiters", IET Energy Syst. Integr., 2020, vol. 2 issue 1, pp. 59-65.
- [6] Mahmoud, R. A., and Malik, O. P. "Adaptive overcurrent relay (AOCR) based on Fano Factors of current signals", IET The journal of Engineering 2023, e12267 (2023). <https://doi.org/10.1049/tje2.12267>.
- [7] Andreev, M., Suvorov, A., Ruban, N., Ufa, R., Gusev, A., Askarov, A., Kievets, A., and Bhalja, B. R. "Settings determination for numerical transformer differential protection via its detailed mathematical model", IET Gener. Transm. Distrib., 2020, vol. 14 issue 10, pp. 1962-1972.
- [8] Zare, J., and Azad, S. P. "A new relaying scheme for protection of transmission lines connected to DFIG-based wind farms", IET Renew. Power Gener. 15, 2971–2982 (2021), <https://doi.org/10.1049/rpg2.12232>.
- [9] Mahmoud, R. A. "Integrated busbar protection scheme utilizing a numerical technique based on coherence method", Journal of Engineering 2022, 94–119 (2022). <https://doi.org/10.1049/tje2.12100>.
- [10] Rajput, V. N., Adelnia, F., and Pandya, K. S. "Optimal coordination of directional overcurrent relays using improved mathematical formulation", IET Gener. Transm. Distrib., 2018, vol. 12 issue 9, pp. 2086-2094.
- [11] Soleimanisardoo, A., and Karegar, H. K. "Alleviating the impact of DGs and network operation modes on the protection system", IET Gener. Transm. Distrib., 2020, vol. 14 issue 1, pp. 21-28.

